HHS Public Access

Author manuscript

Hypertension. Author manuscript; available in PMC 2018 August 01.

Published in final edited form as:

Hypertension. 2017 August ; 70(2): 347–356. doi:10.1161/HYPERTENSIONAHA.116.08871.

Functional TASK-3-like channels in mitochondria of aldosterone producing zona glomerulosa cells

Junlan Yao[a], **David McHedlishvili**[a], **William E. McIntire**[a], **Nick A. Guagliardo**[a], **Alev Erisir**[b], **Craig A. Coburn**[c], **Vincent P. Santarelli**[d], **Douglas A. Bayliss**[a], and **Paula Q. Barrett**[a,#]

[a]Department of Pharmacology, University of Virginia School of Medicine, Charlottesville, VA 22947

[b]Department of Psychology, University of Virginia School of Medicine, Charlottesville, VA 22947

[c]Silverback Therapeutics, Inc., Seattle, WA 98109

[d]Department of Neuroscience, Merck & Co, Inc, West point, PA 19486

Abstract

Ca^{2+} drives aldosterone synthesis in the cytosolic and mitochondrial compartments of the adrenal zona glomerulosa (ZG) cell. Membrane potential across each of these compartments regulates the amplitude of the Ca^{2+} signal; yet, only plasma membrane ion channels and their role in regulating cell membrane potential have garnered investigative attention as pathological causes of human hyperaldosteronism. Previously, we reported that genetic deletion of TASK-3 channels from mice produces aldosterone excess in the absence of a change in the cell membrane potential of ZG cells. Here, we report using yeast two-hybrid, immunoprecipitation and electron microscopic analyses that TASK-3 channels are resident in mitochondria, where they regulate mitochondrial morphology, mitochondrial membrane potential (mitoVm) and aldosterone production. This study provides proof-of-principle that mitochondrial K^+ channels, by modulating inner mitochondrial membrane morphology and mitoVm, have the ability to play a pathological role in aldosterone dysregulation in steroidogenic cells.

Keywords

zona glomerulosa; hyperaldosteronism; leak potassium channels; mitochondria; membrane potential

Ca^{2+} is a critical signal for adrenal and gonadal steroid synthesis[1] acting within two cellular compartments; Ca^{2+} is generated in the cytosol[2,3] and transferred to the mitochondria[4-7] where it activates matrix dehydrogenases to generate reducing equivalents (NAD(P)H) that are essential cofactors for steroid hydroxylation[8]. In aldosterone producing zona glomerulosa (ZG) cells of the adrenal cortex, the dominant pathway for extracellular Ca^{2+}

[#]Corresponding author and person to whom reprint request should be addressed: Paula Q. Barrett, Ph.D., Department of Pharmacology, 1340 Jefferson Park Avenue, Charlottesville, Virginia 22908-0735, Tel: 434-924-5454, Fax: 434-982-3878, pqb4b@virginia.edu.

Disclosures: None

entry into the cytoplasmic compartment are plasma membrane voltage-gated Ca^{2+} channels,[9] whereas the principal pathway for mitochondrial Ca^{2+} uptake is via the mitochondrial uniporter, a Ca^{2+} selective channel[10]. Membrane voltage across each of these compartments regulates Ca^{2+} transport and thus, the rate of steroid production. Because other ion channels resident in each membrane (plasma, mitochondrial) can change membrane voltage, they too are capable of altering Ca^{2+} uptake by mitochondria[11]. Accordingly, it is not surprising that genetic variation in genes encoding ion channels and transporters is now considered central to the pathophysiology of one common subtype of primary hyperaldosteronism (PA), unilateral aldosterone producing adenoma (APA)[12]. In APA, aldosterone synthesis is not strictly controlled by the renin–angiotensin II system, and thus is characterized by a large increase in the aldosterone/renin ratio[13]. Yet, the etiology of other common endocrine hypertensive disorders in which aldosterone production is inappropriate for the level of renin, such as bilateral adrenal hyperplasia (BAH) and low renin essential hypertension (LREH)[14,15], still remains poorly understood.

Our laboratory and that of Barhanin, Warth and colleagues have generated mouse models of aldosterone overproduction evoked by deletion of leak potassium channels that generate background currents to establish a negative resting cell membrane voltage[16-20]. The combined deletion of TASK-1 and TASK-3 channels leads to excessive aldosterone overproduction and low renin in mice. By contrast, deletion of TASK-3 alone evokes mild-hyperaldosteronism and low renin[19], whereas that of TASK-1 elicits mild-hyperaldosteronism without an accompanying suppression of renin[21]. Genetic variations in the human TASK-1 gene (*KCNK3*)[21-23] are associated with measures of hypertension (rs1275988, rs13394970) and elevated plasma aldosterone (rs2586886), and KCNK3 mRNA is abundantly expressed in mouse and human adrenal cortex[24]. By contrast, the KCNK9 gene product, TASK-3, is principally expressed in the rodent adrenal cortex[25], although low levels of message are detected in the human adrenal cortex[26]. The function of TASK-3 in adrenal cortical cells remains unknown.

We previously reported that global deletion of TASK-3 in mice produces a mild hyperaldosteronism even though the cell membrane voltage of ZG cells was not depolarized[19]. Deletion of TASK-3 channels was also not accompanied by a compensatory increase in the expression of other K channels (TASK-1 or Kcnj5) or aldosterone synthase (Cyp11β2). Thus the molecular mechanism underlying aldosterone overproduction in TASK-3-deleted mice has remained unsolved[19]. Motivated by these findings, we investigated the possibility that TASK-3 may exert its control of steroidogenesis in mitochondria. Here, we use three independent methods – yeast two-hybrid, immune-precipitation and electron microscopy – to show that TASK-3 channels reside in mitochondria. Functionally, TASK-3 channel activity regulates mitoVm and aldosterone production. Our studies provide the framework for the possibility that genetic variation in mitochondrial ion channels could underlie subtypes of hyperaldosteronism that have remained unexplained to date.

Methods

Cell culture and chemicals

H295R cells (human adrenocortical carcinoma cells) were cultured in Dulbecco's modified Eagle's medium (DMEM)/F12 containing 10% cosmic calf serum (Hyclone), 1 μg/ml gentamicin. HEK 293T cells (human embryonic kidney cells) were cultured in DMEM/F12 supplemented with 10% fetal bovine serum, 1% pen/strep[27]. The cells were incubated in a 5% CO_2 humidified air incubator at 37°C. HEK 293T cells were transiently transfected with plasmids for TASK-3 channel by using lipofectamine 2000 reagent (Invitrogen) and used for patching 16hrs after transfection. Compound 23 was provided by Merck. Angiotensin II was purchased from Bachem. All other chemicals were obtained from Sigma.

Statistical analysis

Multiple comparisons were evaluated by 1-way ANOVA with Bonferroni multiple comparison post hoc testing (Figures 3B; 4, 6). Significance was determined at $P<0.05$.

See supplemental information for detailed description of all methods.

Results

Yeast two-hybrid analysis and immune-precipitation identifies mitochondrial TASK-3 interaction partners

We commissioned Dualsystems Biotech to perform a yeast-based screen to identify interactions of transmembrane proteins with TASK-3 channels. In this assay, reconstitution of split-ubiquitin (N_{ub}- and C_{ub}-terminal halves) is used as a sensitive sensor of bait-prey contact. In our screen, full-length rat TASK-3, expressed as a fusion to C_{ub} and LexA-VP16 (an artificial transcription factor), was used as bait. The prey, expressed as a fusion to N_{ub}, was a mouse adult brain cDNA library (complexity: 3×10^6 colony-forming units, average size: 1.3 kb). Reconstitution of split-ubiquitin by transmembrane bait-prey contact permitted recognition by ubiquitin-specific proteases, release of LexA-VP16 and subsequent activation of *HIS3* and *ADE2* reporter genes to provide a readout of N_{ub}-C_{ub} reassociation. From 3.6×10^6 transformants, 93 primary clones displayed adenine/histidine prototrophy and β–galactosidase activity. From 84 colonies, plasmid was recovered, amplified in *E.coli* and sequenced. Surprisingly, among the 12 prey proteins encoded by more than 2 cDNAs, nearly half (5) were mitochondrial (Figure 1A). Components of the mitochondrial electron transport chain were among the top hits from the screen (complex 1: NADH-ubiquinone oxidoreductase, complex V: ATP synthase subunit A1), unexpected interaction partners for a K^+ channel that was heretofore considered resident only on plasma membranes.

Motivated by these unexpected findings, we used immune-precipitation to search for TASK-3 binding partners in adrenal glands. Using a custom affinity-purified anti-TASK-3 polyclonal antibody[28] cross-linked to protein-A beads, TASK-3 was immunoprecipitated from 1% CHAPS clarified adrenal lysates from WT and TASK-3-deleted mice. Gel-purified (4-15% SDS-PAGE, non-reducing) immune complexes (Figure 1B) were analyzed by mass spectrometry (LC/MS/MS). Proteomic results were filtered on the basis of peptide coverage.

Listed in Figure 1C are proteins for which at least three unique peptides were identified by LC/MS/MS in WT samples and for which the peptide ratio WT/TASK-3KO was three or greater. Putative TASK-3-interaction partners were grouped on the basis of their molecular functions- steroidogenic or cytoskeletal. As in the Y2H genetic assay, mitochondrial proteins were well represented among the TASK-3-interacting proteins identified biochemically. Included in the top hits were Cytochrome $P450_{SCC}$ (WT/TASK-3KO =9), an inner membrane mitochondrial protein in adrenal and gonadal tissues that catalyzes the rate-limiting step in steroid synthesis; and pyruvate carboxylase (WT/TASK-3KO =7), a matrix ligase that catalyzes the conversion of pyruvate to oxaloacetate. Notably, three additional mitochondrial proteins with peptide recovery ratios of 3 (NADH-ubiquinone oxidoreductase, mitochondrial phosphate carrier protein, and ATP synthase subunit A), were identified that also turned up in the Y2H screen. In addition, mitochondrial inner membrane proteins were identified in a proteomic analysis of TASK-3-containing immune-complexes recovered from human embryonic kidney cells (HEK 293) overexpressing TASK-3, (supplemental Figure S1). Thus, in three different cellular systems using two distinct experimental approaches, mitochondrial proteins were revealed as TASK-3 interaction partners, raising the possibility that TASK-3 channels are located in mitochondria.

Subcellular Distribution of TASK-3 antigen/channels

We used immunoelectron microscopy to study the spatial distribution of TASK-3 channels at the ultrastructural level. Adrenals were fixed and processed for EM and ultrathin sections (60 nm) used in post-embedding immunohistochemistry (anti-TASK-3 primary, anti-rabbit secondary conjugated with 15 nm colloidal gold particles). We used systematic uniform random sampling within a grid for image capture, acquiring 30 high-resolution images from each genotype (from 3 mice each). In representative EM images of the ZG layer from WT mice, gold particles were associated with mitochondria (Figure 2A-C). By contrast, few gold particles were observed in images of ZG cells from TASK-3KO mice (Figure 2D-F).

In order to determine the selectivity of immno-gold particles for mitochondria, we used previously established counting procedures[29], and compared the distribution and the density (particles/area) of gold particles associated with mitochondria, non-mitochondrial areas including the plasma membrane (residuum) and the nucleus. Two researchers blinded to the genotype of the tissue independently counted gold particles in 60 electron micrographs and determined the area of occupying compartments by superimposing a uniform array of test points (0.33 μm spacing) and then recording the number of points that overlaid each compartment. We observed: 1. nearly 10× more particles in WT than TASK-3 KO ZG cells (1137 versus *191* respectively*),* corroborating TASK channel deletion and immune-specificity (Figure 3A); and 2. immuno-labeling was preferentially observed in the mitochondrial compartment. Gold particles associated with mitochondria in WT ZG cells were more abundant than would be expected (N,obs versus N,exp, Figure 3A) if particles were ubiquitously distributed on the section surface. Thus, a 2-fold increase in surface particle density was observed for the mitochondrial compartment that was not observed for either the nucleus or the residuum (Figure 3B). By contrast, the low number of gold particles associated with TASK-3 KO mitochondria was as expected and is in agreement with an evenly distributed non-specific signal (Figure 3A-B). Quantification of surface particle

density associated with plasma membranes (designated as “surface occupying compartment” in this analysis[29]) was obtained by measuring the length of plasma membrane and counting the particles located on or touching the membrane. The labeling intensity was expressed as gold-particle count/10 micron length of membrane. The labeling intensity was low on the plasma membrane of WT ZG (139 particles/432 micrometers of total membrane measured). This low detection on plasma membranes may explain the lack of difference in membrane potential between TASK-3 KO and WT ZG cells recorded in mouse rosettes, as previously reported[19]. Nevertheless, gold-particle density was greater in WT than TASK-3 KO cells (gp/10μm WT: 3.2±0.3 vs. KO: 0.5±0.2, $P \leq 0.02$, Figure 3C), indicating some specific but functionally inconsequential antigen localization to the plasma membrane.

We noted that mitochondrial morphology changed with TASK-3 deletion (Figure 2D-F). TASK-3 KO mitochondria are larger than WT, as indicated by the right-ward shift in the distribution of mitochondrial area and the greater mean area (KO: 0.17±0.07 μm^2 vs. WT: 0.10±0.06 μm^2, $P \leq 0.05$, Figure 4A). However, the maximum and minimum diameters of TASK-3 KO mitochondria were proportionally larger, yielding a similar aspect ratio ($Feret_{min}/Feret_{max}$ KO: 0.77±0.01 versus WT: 0.72±0.01, n.s., Figure 4B-C). Thus, the dynamic processes of mitochondrial fusion (elongation) or fission (fragmentation), which typically alter aspect ratio[30], do not appear to be disrupted in KO ZG cells.

In addition to the larger size, TASK-3 KO mitochondria show a striking change in *cristal morphology* (*see*, Figure 2). Unlike WT mitochondria in which tubular cristae are stabilized in the “orthodox-configuration” (i.e., scalloped with alternating repeats of distension and constriction), most TASK-3 KO cristae are captured in an “aggregated configuration” (i.e., appearing as tubular/lamellar structures)[31,32]. Importantly, in adrenal mitochondria an orthodox-to-aggregated transition is indicative of increased mitochondrial ATP synthesis or Ca^{2+} transport[33]. These morphological changes suggest a functional role for TASK-3 channels in mitochondria.

Human adrenal cortical cells (H295R) as a test system for assessing TASK-3 function in mitochondria

We assayed TASK-3 mRNA levels by qRT-PCR in the human adrenal carcinoma cell line, H295R, and compared TASK-3 gene expression with that in HEK-293T cells and native adrenal tissue (microdissected zona glomerulosa layer). We found ample representation of the TASK-3 amplicon in H295R cDNA (Figure 5A). Relative gene expression was ~240× more than that in HEK293T cells but ~100× less than that in native mouse ZG tissue (Figure 5B), consistent with the quantitative disparity in levels of TASK-3 expression previously report in mouse and human adrenals[26].

To establish if TASK-3 is functionally active on H295R cell plasma membranes, we used a novel TASK-3 antagonist compound C23 (C23) modeled on 5,6,7,8-tetrahydropyrido[4,3-*d*]pyrimidine[34]. C23 shows good selectivity for TASK-3 over other two-pore domain K^+ channels, and a potency of 35 nM (IC_{50} for current inhibition)[34]. We corroborated current inhibition by C23 in HEK293T cells heterologously expressing recombinant rTASK-3 channels. TASK-3 currents rectified weakly, reversed near the expected E_K (~-80 mV), and were pH-sensitive (inhibited by pH 5.9) (Figure 5C). As reported, C23 from 1 to 500 nM

dose-dependently inhibited recombinant TASK-3 currents although unexpectedly current inhibition was incomplete (Figure 5D). By these criteria, whole cell currents elicited by identical voltage ramp protocols in H295R cells were not TASK-like: outward currents were either exceptionally small (type 2) or sharply rectifying with a reversal potential positive to –50 mV (type 1), and neither current type was inhibited by C23 (Figure 5E). In agreement with the overall lack of TASK-like currents in H295R cells, resting membrane potential was depolarized (Vm-before: -20 to +10 mV, Figure 5F, closed circles), and refractory to reduction by 100 nM C23 (Vm-after). C23 was also ineffective at hyperpolarized potentials when current injection was used to shift membrane potential into the more negative voltage range characteristic of native ZG cells[35]. Thus, despite expressing TASK-3 mRNA, H295R cells have no recordable TASK-like whole-cell membrane currents, raising the intriguing possibility that TASK-3 may function sub-cellularly.

TASK-3 modulates mitoVm and aldosterone production

We used JC-10, a cationic mitochondrial selective probe, to monitor changes in mitoVm elicited by Ang II and/or C23. JC-10 accumulates in the mitochondrial matrix upon membrane polarization and shifts its fluorescence emission wavelength from green to yellow[36]. Thus, an increase in relative emission ratio (576/544) provides a useful and relative index of mitoVm hyperpolarization. Ang II (10 nm) evoked a rapid rise in mitoVm in H295R cells that further increased slowly over a 20 minute recording period. By contrast, C23 elicited slow time-dependent changes in mitoVm that depended on dose but that ultimately attained a degree of mitoVm polarization that was similar to that elicited by Ang II (Figure 6A). In agreement with the mitochondrial origin of these signals, the prototypical mitochondrial uncoupler, FCCP, or the novel protonophore BAM 15 that lacks cytotoxic off-target effects (Supplemental Figure S2)[37] depolarized mitoVm (i.e., decreased JC-10 yellow fluorescence). Moreover, in adrenal cells previously stimulated with Ang II, C23 challenge (2nd addition) did not further increase mitoVm polarization, suggesting that either a maximal degree of mitoVm polarization was evoked by each or that, like C23, Ang II may functionally inhibit mitoTASK channels (Figure 6A).

If mitoVm polarization is part of the mechanism by which Ang II stimulates aldosterone production, then C23 alone should also stimulate steroidogenesis in H295R cells that express TASK-3 message but lack plasma membrane TASK channels (see, Figure 5). We measured aldosterone produced from H295R cells evoked by Ang II (10 or 500 nM) or C23 (100 or 500 nM; near-maximal and supramaximal respectively) alone and in combination. As expected, Ang II dose-dependently increased the production of aldosterone, and evoked greater maximal stimulatory responses at 24 hours (3.3-fold versus 30-fold) consistent with its well-known effect to increase CYP11β2 transcription. By contrast, stimulation of aldosterone production by C23 was equivalent at 6 and 24 hrs (~3-fold). As a consequence, C23 was one-tenth as effective as Ang II at regulating the sustained production of aldosterone (Figure 6B).

To determine if C23 and Ang II regulate aldosterone secretion by mutually exclusive mechanisms, we evaluated the additivity of elicited responses during co-stimuation. We found that C23 modestly increased Ang II-stimulated aldosterone secretion from H295R

cells with submaximal doses of Ang II (1.2- versus 1.9-fold at 6 and 24 hrs. respectively) well below the magnitude predicted from additivity (5.1- versus 10.3-fold, Figure 6C). In addition, C23 failed to potentiate responses to maximally effective doses of Ang II at either time point, suggesting a shared event (i.e. mitoVm polarization) in the steroidogenic action of these agonists. Regulation of aldosterone production by C23 was also demonstrable in slices prepared from native adrenal tissue; C23 stimulated aldosterone production from wild-type slices, but was without effect in slices prepared from mice deleted for both TASK-1 and TASK-3 (Figure 6D). Taken together these data highlight the functional role of mitochondrial ZG TASK-3 channels in the control of aldosterone production in native and cell cultured systems.

Discussion

In this study we found, using both genetic (Y2H) and biochemical analyses (IP and MS/MS), that TASK-3 channels interact with mitochondrial inner membrane proteins of the electron transport chain and additionally, in steroidogenic tissue, steroid hydroxylating P450cytochromes. TASK-3 channels within the ZG layer also were detected by immune-electron microscopy in mitochondria of WT but not TASK-3 KO adrenal glands at an abundance that was disproportionate to the spatial area occupied by the mitochondrial subcellular compartment. Together, these data argue that TASK-3 channels can be sorted to mitochondria in steroidogenic cells, extending findings of an earlier report documenting TASK-3 channel expression in mitochondria of melanoma malignum cells[38]. Although TASK-3 is missing a discrete amino terminal mitochondrial targeting sequence, many proteins that lack such a signal are imported to mitochondria by internal targeting sequences or cytosolic chaperone proteins[39].

As members of the *KCNK* gene family, TASK-3 channels are “leak” conductances that generate “background” currents and are widely expressed in both excitable and non-excitable cells. On the plasma membrane, they prominently function to produce negative resting membrane voltages[40]. As putative residents of the inner-mitochondrial membrane, they join a select group of K^+-selective channels including mitoKATP (K_{ir} 6.1/6.2), mitoBK$_{Ca}$ (slo 1), and mitoKv1.3 that display properties similar to their cognate channels on the plasma membrane[11]. By increasing K^+ influx into mitochondria and hence reducing mitochondrial membrane potential (mitoVm), mitoK^+ channels in cardiac and neuronal cells defend against ischemic injury and neuronal toxicity[11,41] at least in part by reducing mitochondrial Ca^{2+} uptake.

We present three pieces of evidence that support a functional role for TASK-3 channels in adrenal mitochondria. First, a greater proportion of mitochondria in TASK-3 KO ZG cells have expanded intracristal spaces. In the adrenal cortex, the topology of the cristae membrane (involutions of the inner mitochondrial membrane) dynamically changes with the physiological state of the cell[32]. The condensed configuration characterized by tubular lamellae is more prevalent in TASK-3 KO mitochondria and is associated with (and presumably supports) an increased capacity to translocate Ca^{2+} [33]. Second, the TASK-3 antagonist, C23, hyperpolarizes mitoVm in an adrenal model cell that lacks functional TASK plasma membrane channels. These data indicate a TASK-3-like conductance in the

mitochondrial inner membrane. Third, we find that the pharmacological inhibition of TASK-3 activity also stimulates aldosterone production. Stimulation occurs in native WT adrenal tissue, but not in tissue lacking TASK-1 and TASK-3 channels. Notably, stimulation of production also is demonstrable in the model human adrenal cell, H295R, in which mitoVm, but not plasma membrane Vm, is altered by C23. Thus, by both morphological and bioenergetic measures TASK-3-like channels in adrenal mitochondria are functional.

We note that in the normal human adrenal, there is a large difference in TASK-3 expression detected between adrenal layers; TASK-3 mRNA is found in the human ZG but at 100-fold lower levels than in the ZM[26]. We also find low levels of TASK-3 mRNA in H295R cells (~100-fold less abundant than in rodent ZG). Nevertheless, mitoTASK-3 activity was able to regulate mitoVm in H295R cells. In addition, we observed that the absolute loss of TASK-3 expression produced striking effects on cristae structure in rodent ZG; it remains to be determined if low TASK-3 expression in normal human ZG influences mitochondrial morphology.

Although TASK-3 channels generate a “leak” current, there are well established mechanisms for their regulation. TASK-3 channels are inhibited by extracellular hydrogen ions (pK~6.8) and by heterotrimeric G_q activation. However, high extracellular [K^+], as occurs in the cytosol[42], antagonizes H^+-mediated channel inhibition[43] and Gαq, although resident on the inner mitochondrial membrane, is not complexed with Gβγ dimers[44], indicating that mitochondrial Angiotension type 1 receptors (AT1R)[45] could not regulate TASK-3 channels by a mechanism analogous to that evoked by AT1Rs at the plasma membrane. Thus, in mitochondria other mechanisms may exist for TASK channel regulation.

We also report here that Ang II, the major regulator of aldosterone production from ZG cells, evokes hyperpolarization of mitoVm. Whether this action is dependent on TASK-3 channels is not addressed in this study but remains an intriguing possibility. Nevertheless, the failure of C23 to augment aldosterone production evoked by maximally effective doses of Ang II and regulate production from wild-type but not TASK deletion slices suggests that mitoVm polarization is one part of the mechanism by which Ang II regulates aldosterone production. A hyperpolarization of the mitoVm, would contribute to increasing mitoCa uptake, and NADH generation, well known mitochondrial actions of Ang II that drive steroidogenesis. Finally, we note parenthetically a recent report documenting a consistent blunted expression of a related *KCNK* family member, TASK-2, in aldosterone producing adenomas of the adrenal cortex[46]. Whether genetic variation in mitochondrial K^+ channels, like that of plasma membrane K^+ channels, drives disorders of aldosterone production warrants consideration and investigation.

Perspectives

Cholesterol side-chain cleavage enzyme and aldosterone synthase catalyze rate-limiting steps in aldosterone biosynthesis. Their activities depend on NADPH, a cofactor made using the energy of mitoVm: the electrical component driving Ca^{2+}-dependent matrix dehydrogenase activity with consequent NADH formation, and the proton component driving NAD(P)-transhydrogenase activity with subsequent NADPH formation. Here, we

show that in steroidogenic cells, TASK-3 leak K^+ channels are functional mitochondrial ion channels regulating cristal morphology, mitoVm and aldosterone biosynthesis. By partially depolarizing mitoVm, the physiological role of mitoTASK channels may be to limit steroidogenesis in adrenal cortical cells and thus protect against excessive electron leakage produced from steroid hydroxylation.

Supplementary Material

Refer to Web version on PubMed Central for supplementary material.

Acknowledgments

Drs. M. Okusa and D. Rosin for use of the MBF Bioscience and Zeiss microscope system, Dr. Kyle Hoehn for supplying BAM 15.

Sources of Funding: This study was supported by NHLBI grant R01 HL089717 to P.Q.B. and D.A. Bayliss. Morphometric analysis was determined on “MBF Bioscience and Zeiss microscope system for stereology and tissue morphology” funded by National Institutes of Health Grant 1S10RR026799-01 (MD Okusa, PI).

References

1. Papadopoulos V, Miller WL. Role of mitochondria in steroidogenesis. Best Pract Res Clin Endocrinol Metab. 2012; 26:771–790. [PubMed: 23168279]
2. Clark BJ, Pezzi V, Stocco DM, Rainey WE. The steroidogenic acute regulatory protein is induced by angiotensin ii and k+ in h295r adrenocortical cells. Mol Cell Endocrinol. 1995; 115:215–219. [PubMed: 8824897]
3. Cherradi N, Rossier MF, Vallotton MB, Timberg R, Friedberg I, Orly J, Wang XJ, Stocco DM, Capponi AM. Submitochondrial distribution of three key steroidogenic proteins (steroidogenic acute regulatory protein and cytochrome p450scc and 3beta-hydroxysteroid dehydrogenase isomerase enzymes) upon stimulation by intracellular calcium in adrenal glomerulosa cells. J Biol Chem. 1997; 272:7899–7907. [PubMed: 9065457]
4. Rossier MF, Burnay MM, Brandenburger Y, Cherradi N, Vallotton MB, Capponi AM. Sources and sites of action of calcium in the regulation of aldosterone biosynthesis. Endocr Res. 1996; 22:579–588. [PubMed: 8969915]
5. Pitter JG, Maechler P, Wollheim CB, Spat A. Mitochondria respond to ca2+ already in the submicromolar range: Correlation with redox state. Cell Calcium. 2002; 31:97–104. [PubMed: 11969250]
6. Lalevee N, Resin V, Arnaudeau S, Demaurex N, Rossier MF. Intracellular transport of calcium from plasma membrane to mitochondria in adrenal h295r cells: Implication for steroidogenesis. Endocrinology. 2003; 144:4575–4585. [PubMed: 12960050]
7. Spat A, Pitter JG. The effect of cytoplasmic ca2+ signal on the redox state of mitochondrial pyridine nucleotides. Mol Cell Endocrinol. 2004; 215:115–118. [PubMed: 15026183]
8. Wiederkehr A, Szanda G, Akhmedov D, Mataki C, Heizmann CW, Schoonjans K, Pozzan T, Spat A, Wollheim CB. Mitochondrial matrix calcium is an activating signal for hormone secretion. Cell Metab. 2011; 13:601–611. [PubMed: 21531342]
9. Barrett PQ, Guagliardo NA, Klein PM, Hu C, Breault DT, Beenhakker MP. Role of voltage-gated calcium channels in the regulation of aldosterone production from zona glomerulosa cells of the adrenal cortex. J Physiol. 2016; 594:5851–5860. [PubMed: 26845064]
10. Kirichok Y, Krapivinsky G, Clapham DE. The mitochondrial calcium uniporter is a highly selective ion channel. Nature. 2004; 427:360–364. [PubMed: 14737170]
11. Szewczyk A, Skalska J, Glab M, Kulawiak B, Malinska D, Koszela-Piotrowska I, Kunz WS. Mitochondrial potassium channels: From pharmacology to function. Biochim Biophys Acta. 2006; 1757:715–720. [PubMed: 16787636]

12. Zennaro MC, Boulkroun S, Fernandes-Rosa F. An update on novel mechanisms of primary aldosteronism. J Endocrinol. 2015; 224:R63–77. [PubMed: 25424518]
13. Montori VM, Young WF Jr. Use of plasma aldosterone concentration-to-plasma renin activity ratio as a screening test for primary aldosteronism. A systematic review of the literature. Endocrinol Metab Clin North Am. 2002; 31:619–632. xi. [PubMed: 12227124]
14. Mulatero P, Bertello C, Verhovez A, Rossato D, Giraudo G, Mengozzi G, Limerutti G, Avenatti E, Tizzani D, Veglio F. Differential diagnosis of primary aldosteronism subtypes. Curr Hypertens Rep. 2009; 11:217–223. [PubMed: 19442332]
15. Young WF. Primary aldosteronism: Renaissance of a syndrome. Clin Endocrinol (Oxf). 2007; 66:607–618. [PubMed: 17492946]
16. Heitzmann D, Derand R, Jungbauer S, et al. Invalidation of task1 potassium channels disrupts adrenal gland zonation and mineralocorticoid homeostasis. EMBO J. 2008; 27:179–187. [PubMed: 18034154]
17. Davies LA, Hu C, Guagliardo NA, Sen N, Chen X, Talley EM, Carey RM, Bayliss DA, Barrett PQ. Task channel deletion in mice causes primary hyperaldosteronism. Proc Natl Acad Sci U S A. 2008; 105:2203–2208. [PubMed: 18250325]
18. Bandulik S, Penton D, Barhanin J, Warth R. Task1 and task3 potassium channels: Determinants of aldosterone secretion and adrenocortical zonation. Horm Metab Res. 2010; 42:450–457. [PubMed: 20049674]
19. Guagliardo NA, Yao J, Hu C, Schertz EM, Tyson DA, Carey RM, Bayliss DA, Barrett PQ. Task-3 channel deletion in mice recapitulates low-renin essential hypertension. Hypertension. 2012; 59:999–1005. [PubMed: 22493079]
20. Bandulik S, Tauber P, Penton D, Schweda F, Tegtmeier I, Sterner C, Lalli E, Lesage F, Hartmann M, Barhanin J, Warth R. Severe hyperaldosteronism in neonatal task3 potassium channel knockout mice is associated with activation of the intraadrenal renin-angiotensin system. Endocrinology. 2013; 154:2712–2722. [PubMed: 23698720]
21. Manichaikul A, Rich SS, Allison MA, Guagliardo NA, Bayliss DA, Carey RM, Barrett PQ. Kcnk3 variants are associated with hyperaldosteronism and hypertension. Hypertension. 2016; 68:356–364. [PubMed: 27296998]
22. Ganesh SK, Chasman DI, Larson MG, et al. Effects of long-term averaging of quantitative blood pressure traits on the detection of genetic associations. Am J Hum Genet. 2014; 95:49–65. [PubMed: 24975945]
23. Kato N, Loh M, Takeuchi F, et al. Trans-ancestry genome-wide association study identifies 12 genetic loci influencing blood pressure and implicates a role for DNA methylation. Nat Genet. 2015; 47:1282–1293. [PubMed: 26390057]
24. Nogueira EF, Gerry D, Mantero F, Mariniello B, Rainey WE. The role of task1 in aldosterone production and its expression in normal adrenal and aldosterone-producing adenomas. Clin Endocrinol (Oxf). 2010; 73:22–29. [PubMed: 19878209]
25. Czirjak G, Enyedi P. Task-3 dominates the background potassium conductance in rat adrenal glomerulosa cells. Mol Endocrinol. 2002; 16:621–629. [PubMed: 11875121]
26. Chen AX, Nishimoto K, Nanba K, Rainey WE. Potassium channels related to primary aldosteronism: Expression similarities and differences between human and rat adrenals. Mol Cell Endocrinol. 2015; 417:141–148. [PubMed: 26375812]
27. Parmar J, Key RE, Rainey WE. Development of an adrenocorticotropin-responsive human adrenocortical carcinoma cell line. J Clin Endocrinol Metab. 2008; 93:4542–4546. [PubMed: 18713819]
28. Berg AP, Talley EM, Manger JP, Bayliss DA. Motoneurons express heteromeric twik-related acid-sensitive k+ (task) channels containing task-1 (kcnk3) and task-3 (kcnk9) subunits. J Neurosci. 2004; 24:6693–6702. [PubMed: 15282272]
29. Mayhew TM, Muhlfeld C, Vanhecke D, Ochs M. A review of recent methods for efficiently quantifying immunogold and other nanoparticles using tem sections through cells, tissues and organs. Ann Anat. 2009; 191:153–170. [PubMed: 19135344]
30. Chan DC. Mitochondrial fusion and fission in mammals. Annu Rev Cell Dev Biol. 2006; 22:79–99. [PubMed: 16704336]

31. Allmann DW, Munroe J, Wakabayashi T, Harris RA, Green DE. Studies on the transition of the cristal membrane from the orthodox to the aggregated configuration. Ii. Determinants of the orthodox-aggregated transition in adrenal cortex mitochondria. J Bioenerg. 1970; 1:87–107. [PubMed: 5005952]
32. Allmann DW, Wakabayashi T, Korman EF, Green DE. Studies on the transition of the cristal membrane from the orthodox to the aggregated configuration. I. Topology of bovine adrenal cortex mitochondria in the orthodox configuration. J Bioenerg. 1970; 1:73–86. [PubMed: 5527907]
33. Allmann DW, Munroe J, Wakabayashi T, Green DE. Studies on the transition of the cristal membrane from the orthodox to the aggregated configuration. 3. Loss of coupling ability of adrenal cortex mitochondria in the orthodox configuration. J Bioenerg. 1970; 1:331–353. [PubMed: 5527911]
34. Coburn CA, Luo Y, Cui M, et al. Discovery of a pharmacologically active antagonist of the two-pore-domain potassium channel k2p9.1 (task-3). ChemMedChem. 2012; 7:123–133. [PubMed: 21916012]
35. Guagliardo NA, Yao J, Hu C, Barrett PQ. Minireview: Aldosterone biosynthesis: Electrically gated for our protection. Endocrinology. 2012; 153:3579–3586. [PubMed: 22689262]
36. Burridge PW, Li YF, Matsa E, et al. Human induced pluripotent stem cell-derived cardiomyocytes recapitulate the predilection of breast cancer patients to doxorubicin-induced cardiotoxicity. Nat Med. 2016; 22:547–556. [PubMed: 27089514]
37. Kenwood BM, Weaver JL, Bajwa A, et al. Identification of a novel mitochondrial uncoupler that does not depolarize the plasma membrane. Mol Metab. 2014; 3:114–123. [PubMed: 24634817]
38. Kosztka L, Rusznak Z, Nagy D, Nagy Z, Fodor J, Szucs G, Telek A, Gonczi M, Ruzsnavszky O, Szentandrassy N, Csernoch L. Inhibition of task-3 (kcnk9) channel biosynthesis changes cell morphology and decreases both DNA content and mitochondrial function of melanoma cells maintained in cell culture. Melanoma Res. 2011; 21:308–322. [PubMed: 21512417]
39. Stojanovski D, Bohnert M, Pfanner N, van der Laan M. Mechanisms of protein sorting in mitochondria. Cold Spring Harbor perspectives in biology. 2012; 4:a011320. [PubMed: 23028120]
40. Bayliss DA, Barrett PQ. Emerging roles for two-pore-domain potassium channels and their potential therapeutic impact. Trends Pharmacol Sci. 2008; 29:566–575. [PubMed: 18823665]
41. O'Rourke B, Cortassa S, Aon MA. Mitochondrial ion channels: Gatekeepers of life and death. Physiology (Bethesda). 2005; 20:303–315. [PubMed: 16174870]
42. Kim Y, Bang H, Kim D. Task-3, a new member of the tandem pore k(+) channel family. J Biol Chem. 2000; 275:9340–9347. [PubMed: 10734076]
43. Gonzalez W, Zuniga L, Cid LP, Arevalo B, Niemeyer MI, Sepulveda FV. An extracellular ion pathway plays a central role in the cooperative gating of a k(2p) k+ channel by extracellular ph. J Biol Chem. 2013; 288:5984–5991. [PubMed: 23319597]
44. Beninca C, Planaguma J, de Freitas Shuck A, Acin-Perez R, Munoz JP, de Almeida MM, Brown JH, Murphy AN, Zorzano A, Enriquez JA, Aragay AM. A new non-canonical pathway of galpha(q) protein regulating mitochondrial dynamics and bioenergetics. Cell Signal. 2014; 26:1135–1146. [PubMed: 24444709]
45. Abadir PM, Foster DB, Crow M, Cooke CA, Rucker JJ, Jain A, Smith BJ, Burks TN, Cohn RD, Fedarko NS, Carey RM, O'Rourke B, Walston JD. Identification and characterization of a functional mitochondrial angiotensin system. Proc Natl Acad Sci U S A. 2011; 108:14849–14854. [PubMed: 21852574]
46. Lenzini L, Caroccia B, Campos AG, Fassina A, Belloni AS, Seccia TM, Kuppusamy M, Ferraro S, Skander G, Bader M, Rainey WE, Rossi GP. Lower expression of the twik-related acid-sensitive k + channel 2 (task-2) gene is a hallmark of aldosterone-producing adenoma causing human primary aldosteronism. J Clin Endocrinol Metab. 2014; 99:E674–682. [PubMed: 24285684]

Novelty and Significance

What is New?

- Leak potassium channels are resident in mitochondria of steroid producing cells.
- These channels are functional, regulating cristal morphology, mitoVm and aldosterone production.

What is Relevant?

Steroid hormone synthesis occurs predominately in mitochondria, and depends upon the membrane potential that is generated across the inner mitochondrial membrane. To date, this control point for regulating steroidogenesis has been largely overlooked. Our study provides proof-of-principle that identifying mitochondrial membrane conductances in steroidogenic cells and mechanisms for their regulation could provide new ways to control excessive/inappropriate steroid synthesis that underlies a spectrum of hypertensive disorders within the syndrome of low renin hypertension.

Summary

Potassium channels on the mitochondrial inner membrane provide a novel pathway for regulating aldosterone secretion in adrenal glomerulosa cells.

A Yeast Two-Hybrid

TASK-3 Interacting Proteins	Uniport ID	# hits
NADH-Ubiquinone oxidoreductase chain 1-5	P03888	14
ATP synthase subunit alpha	Q96064	6
Renin receptor	Q9CYN9	5
Trans-2,3 enoyl-CoA reductase (ER)	Q9CY27	5
4F2 cell-surface antigen heavy chain	P10852	3
Lysosomal-associated transmembrane protein 4B	Q91XQ6	3
Plasma Membrane calcium-transporting ATPase	P23634	3
Stress-association ER protein 2	Q6TAW2	3
Mitochondrial inner membrane protein OXA1L	Q8BGA9	2
Phosphate carrier protein, mitochondrial	Q8VEM8	2
Protein CutA (acetylcholinesterase putative membrane anchor)	Q9CQ89	2
Protoheme IX franesyltransferase, mitochondrial	Q8CFY5	2

B Mouse Adrenal

TASK-3 Interacting Proteins	MW kDa	Peptides		WT: TASK-3 KO
		TASK-3 KO	WT	
Cholesterol side chain cleavage enzyme	60	1	9	9.0
Keratin, type I cytoskeletal 14	53	1	4	4.0
Isoform 1 of Filamin-A	281	2	7	3.5
Pyruvate carboxylase	130	2	7	3.5
NADPH: adrenodoxin oxidoreductase	57	2	6	3.0
3 beta-hydroxysteroid dehydrogenase-Delta 5-->4-isomerase type 1	42	1	3	3.0
Phosphate carrier protein	40	1	3	3.0
Heat shock protein 90 alpha (Cytosolic), class B member 1	83	1	3	3.0
ATP synthase subunit alpha	60	1	3	3.0
Fibrinogen gamma chain	50	1	3	3.0
Tubulin beta-4 chain	50	1	3	3.0
Isoform 1 of Elongation factor Tu	50	1	3	3.0

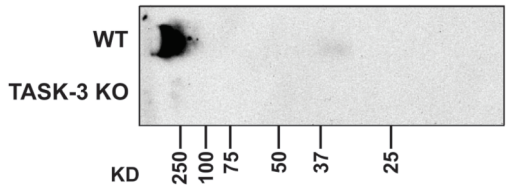

Figure 1. TASK-3 interacts with mitochondrial inner membrane proteins

Mitochondrial binding partners identified by bolded text. **A. Y2H.** TASK-3 interacting proteins identified in a split-ubiquitin membrane yeast two hybrid (Y2H) screen using a transmembrane bait protein library. Identified proteins are ranked by number of "hits". **B. Mouse Adrenals.** ***Left.*** Coomaisse stained SDS-PAGE of immune-precipitates prepared from adrenal lysates (WT and TASK-3 KO) used for LC/MS/MS. ***Right.*** Proteomic analysis of unique peptides recovered from WT and TASK-3 KO immune-precipitates. Ratio of peptide recovery (WT/TASK-3 KO) denotes specificity and retrieves mitochondrial proteins.

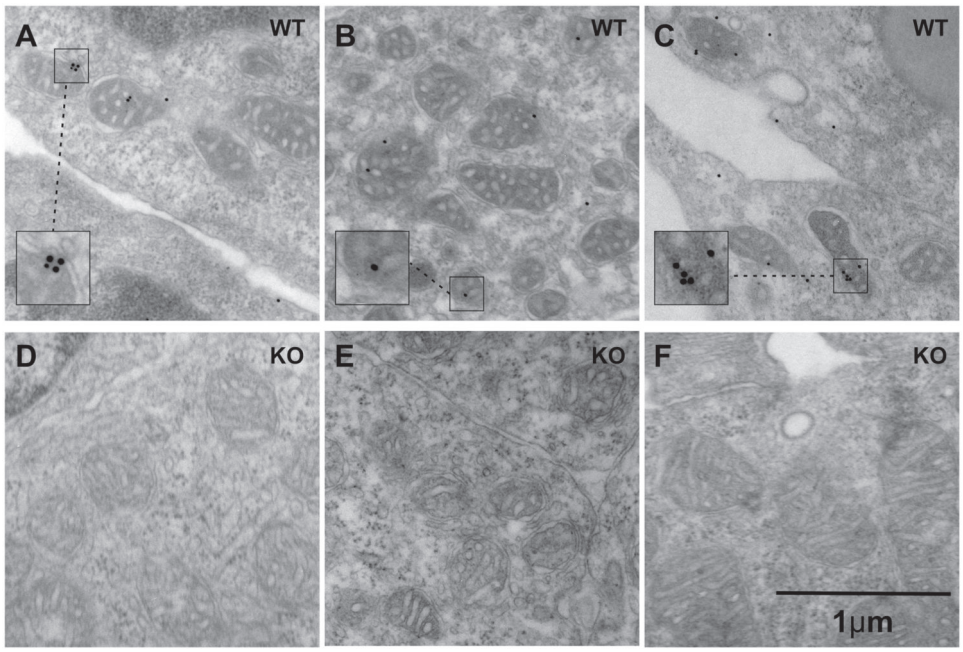

Figure 2. Surface localization of TASK-3 antigen to adrenal mitochondria in the zona glomerulosa (ZG) layer

Representative electron micrographs of TASK-3 immuno-gold labeling of mouse adrenal ZG-layer (n=3 animals, WT (**A-C**) and TASK-3 KO (**D-F**). Boxes surround and expand image area to highlight silver-enhanced gold particles associated with WT mitochondria that are not evident in TASK-3 KO mitochondria.

A

WT	N, obs	Area	N, exp
Compartments	*gold particles*	*test points*	*expected particles*
mitochondria	309	867	147
nucleus	185	1467	249
residuum	643	4358	740
totals	1137	6692	
TASK-3KO	**Nobs**	**Area**	**Nexp**
Compartments	*gold particles*	*test points*	*expected particles*
mitochondria	25	688	20
nucleus	63	1809	53
residuum	103	4033	118
totals	191	6530	

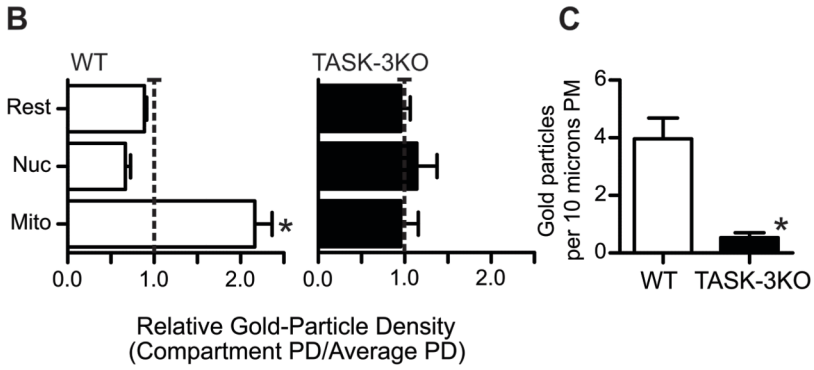

Figure 3. Relative distribution of TASK-3 gold particles in adrenal ZG-layer. A. Nobs (number of observed gold particles)

Cumulative count of silver-enhanced gold particles associated with ZG layer mitochondria, nucleus or residuum in micrographs from each genotype (10 micrographs per adrenal, n=3 animals, WT and TASK-3 KO). **Area (test points)**. Area compartments measured from micrographs determining number of test points that overlay each compartment from a superimposed systematic array (0.33 μm spacing). **Nexp (number of expected gold particles).** Expected distribution of gold-particles per compartment if gold-particles were randomly dispersed ([Total Nobs/Total area test points] × Compartment area test points). **B.** Compartment Density (Nobs/Area) relative to random density (Total Nobs/Total Area) shows selective enrichment of TASK-3 antigen associated with WT mitochondria. **C.** Plasma membrane gold particle density calculated from electron micrographs using morphometric perimeter analysis (Stereo Investigator) showing enhanced gold-particle density associated with WT plasma membranes. *1 way-ANOVA, P<0.05. All WT animals differed from TASK-3 KO.

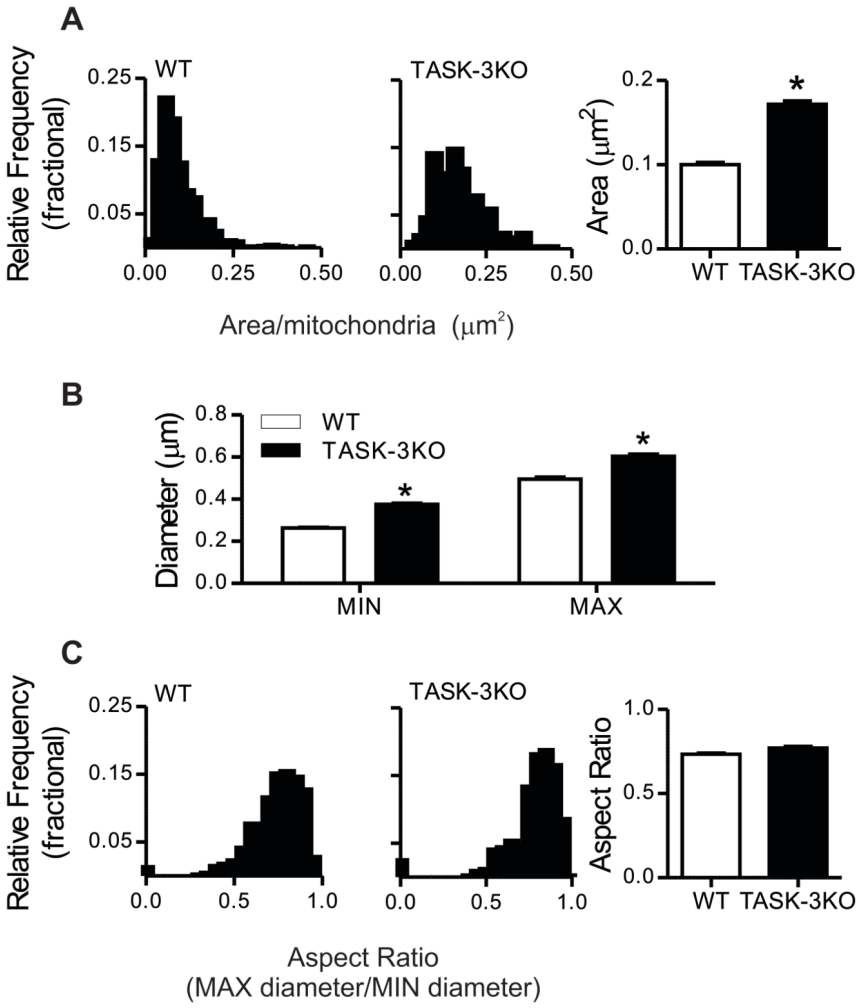

Figure 4. Mitochondrial morphology in ZG layer of WT and TASK-3 KO mice

A. Relative frequency distribution of area per mitochondria (μm^2) measured from electron micrographs (n=3 animals per genotype, 10 micographs per adrenal). TASK-3 deletion increases mitochondrial size. **B.** Both Ferret minimum and maximum diameters are greater in TASK-3 KO mitochondria. **C.** Proportional increases in min and max diameters leaves aspect ratio (max/min diameter) unchanged. *1 way-ANOVA, $P<0.05$. All WT animals differed from TASK-3 KO.

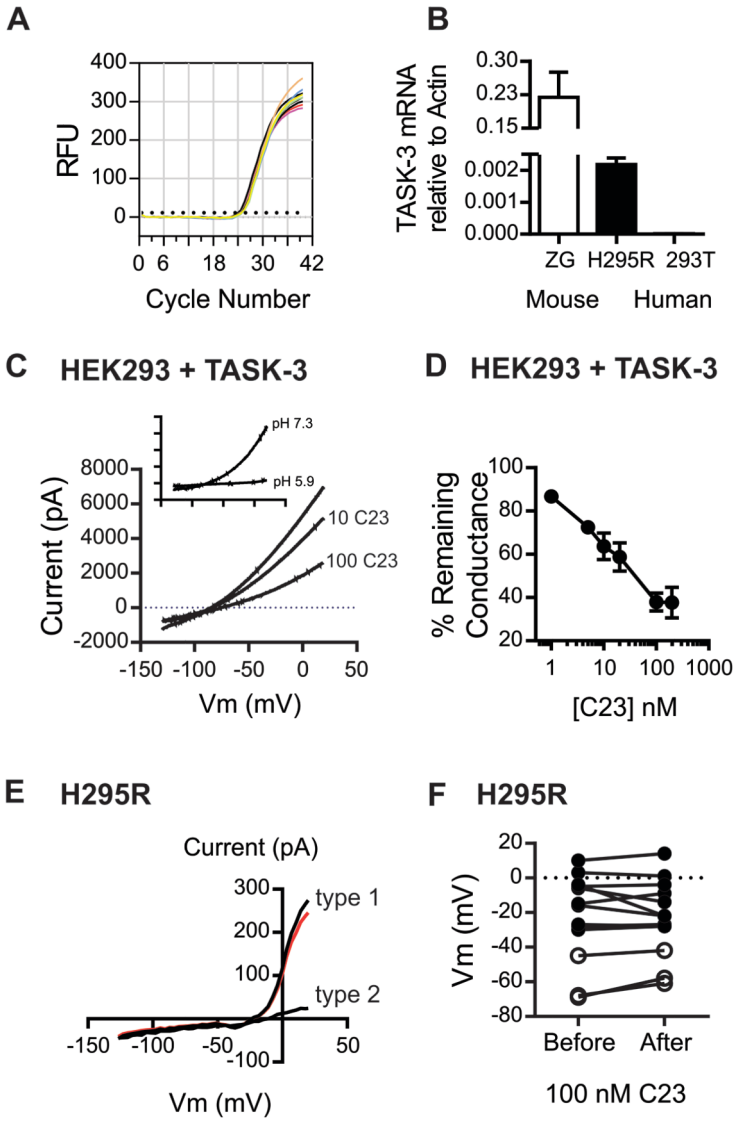

Figure 5. TASK-3 channels in human adrenal cortical cells (H295R) do not control plasma membrane voltage

A. qRTPCR raw signal intensities of TASK-3 mRNA expression in representative H295R samples **B.** Quantification of TASK 3 mRNA by qRT-PCR calculated as $\Delta ct(2^{(ctTASK-ctActin)})$ from micro-dissected mouse ZG layer (n=9), human adrenal cortical (H295R, n=10) or embryonic kidney (HEK293, n=3) cells. **C.** Representative whole-cell voltage-clamp recordings of TASK-3 currents evoked by voltage-ramp protocol (-130 and +20 mV, 0.2V/sec) from HEK293 cells transfected with rTASK-3 constructs. Averaged traces at the onset and after exposure to compound C23 (10, 100 nM). Inset shows inhibition by pH 5.9 for comparison. **D.** Dose-dependence of TASK current inhibition by compound C23. Whole-cell conductance was calculated as the slope of current evoked between -130 and -60 mV. Conductances after 5 min exposure to C23 were normalized by preexposure conductance values (n=35 cells). **E**. Two types of representative whole-cell currents (type 1, type 2) recorded as above in voltage-clamp from H295R cells that are neither TASK-like nor inhibited by C23. Red current trace, type 1 cell current following 5 min exposure to 200 nM

C23. **F.** Current-clamp recordings of H295R cells before and after exposure to C23 (100 nm), showing lack of Vm regulation by TASK-3 (n=13). Open circles denote cells whose Vm was adjusted by hyperpolarizing current injection before C23 exposure (n= 3 cells).

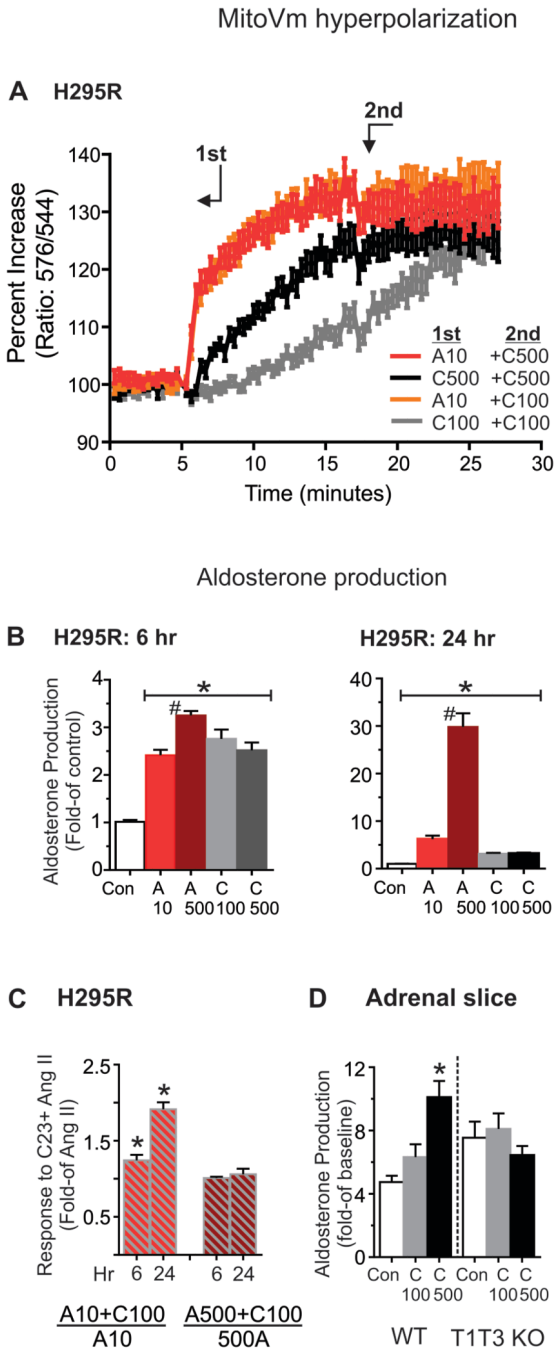

Figure 6. Ang II and C23 hyperpolarize mitoVm and stimulate aldosterone production

A. Ratio of JC-10 fluorescent intensities recorded at 576 and 544 nm; percent increase reporting relative hyperpolarization of mitochondrial membrane potential (mitoVm) in H295R cells. Stimulation with Ang II (10 nM), or C23 (100 or 500 nM) in varied combinations: first agonist addition at 5 min., second at 16.5 min. (24 replicates per condition from 3 cell preparations). **B.** Aldosterone produced from H295R cells expressed as fold-over baseline (n=12, per condition; 3 cell preparations). All agonists added concurrently at t=0. **C**. Fold increase with co-stimulation (10 or 500 nM Ang II with 100 nM C23)

relative to Ang II alone (n≥12, per condition; 3 cell preparations). Note, effects evoked by Ang II and C23 on mitoVm and steroidogenesis are not additive. **D**. Aldosterone production evoked by C23 (100 or 500 nM) from adrenal slices prepared from WT or TASK-1:TASK-3 KO mice expressed as fold-over untreated (n=12 per genotype from 4 adrenals). * 1 way-ANOVA, P<0.05, treatment differed from control; # treatment differed from 10 nM Ang II.